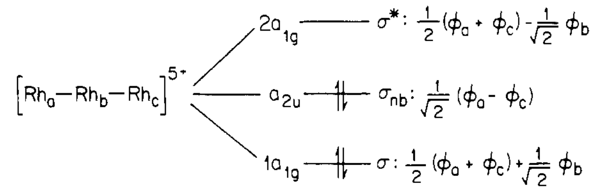

Figure 9. Molecular orbital diagram for linear $[Rh_a{-}Rh_b{-}Rh_c]^{5+}$. See the Figure 6 caption for details.

than the lower energy one, according to Mulliken.[10] If this assignment is correct, the $1a_{1g}$–$2a_{2u}$ splitting is similar to the a_{1g}–a_{2u} separation in d^7–d^7 Rh_2 compounds,[4] which is consistent with the strong central-bond description for the tetramer.

Comparisons to Related Systems

Longer-chain oligomers $[Rh_2b_4]_n^{(2n+2)+}$ have been characterized in solution.[11] The electronic structural model for these complexes closely follows that of the tetramers; a single metal–metal antibonding level is empty in the stable species, and an intense $\sigma \rightarrow \sigma^*$ transition appears at progressively lower energy as n increases.

An interesting additional case is $Rh_n^{(n+2)+}$ with n odd, in particular, the Rh_3^{5+} unit characterized by Balch and Olmstead[12] in the complex $[(C_6H_5CH_2NC)_{12}Rh_3I_2]^{3+}$. The MO diagram for Rh_3^{5+} is shown in Figure 9, where the orbitals are energetically ranked according to the number of nodes (just as for Rh_4^{6+}). The Rh–Rh bond order is $1/\sqrt{2}$ (neglecting overlap), which is consistent with the observed[12] d(Rh–Rh) = 2.796 Å. The only allowed $\sigma \rightarrow \sigma^*$ transition is $a_{2u} \rightarrow 2a_{1g}$, a nonbonding-to-antibonding transition that can also be described as outer → inner rhodium charge transfer. The observed wavelength (525 nm)[12] for the reported intense visible absorption seems reasonable for this description. (It is intermediate between the wavelengths of the bands observed for the I^- adducts of Rh_4^{6+} (Table I) and Rh_2^{4+}.[4])

A final comparison of interest is odd-electron linear-chain systems such as the platinum blues. The intense visible absorption exhibited by these materials is likely to be closely analogous to the bands under scrutiny here. A detailed experimental and theoretical study[13] of one of these materials, that containing *cis*-$[Pt(NH_3)_2(C_5H_4NO)]_4^{5+}$, is in essential agreement, although the much lower symmetry, which allows mixing among σ, π, and δ symmetry orbitals, complicates the analysis. An intense chain-polarized band at 680 nm can be assigned to a $\sigma \rightarrow \sigma^*$ transition corresponding to $2a_{1g} \rightarrow 2a_{2u}$ (Figure 6) in a hypothetical Rh_4^{5+} analogue. It is noteworthy that the geometry of the platinum tetramer, with central and outer bond lengths of 2.877 and 2.775 Å, respectively, implies $\beta > 1$ in our simple MO scheme. However, the fact that both Pt–Pt distances in the platinum tetramer are considerably longer than that of a d^7–d^7 analogue, $[Pt_2(NH_3)_4(C_5H_4NO)_2Cl_2](NO_3)_2$ with d(Pt–Pt) = 2.568 Å,[14] indicates that the Pt–Pt bonds are relatively weak. The platinum compounds appear to fall into a class of inherently shorter metal–metal bonds (for a given bond order) discussed by us elsewhere.[15] Accordingly, the small inner–outer bond length differences found in the tetranuclear platinum ion may not be relevant to the metal–metal bonding situation that prevails for the Rh_4^{6+} compounds.

Acknowledgment. We thank Woody Woodruff for several helpful discussions, especially ones in connection with ref 6. This research was supported by National Science Foundation Grant CHE84-19828.

(10) Mulliken, R. S. *J. Chem. Phys.* **1939**, *7*, 121–135.

(11) (a) Sigal, I. S.; Mann, K. R.; Gray, H. B. *J. Am. Chem. Soc.* **1980**, *102*, 7252–7256, (b) Sigal, I. S.; Gray, H. B. *J. Am. Chem. Soc.* **1981**, *103*, 2220–2225.

(12) Balch, A. L.; Olmstead, M. M. *J. Am. Chem. Soc.* **1979**, *101*, 3128–3129.

(13) Ginsberg, A. P.; O'Halloran, T. V.; Fanwick, P. E.; Hollis, L. S.; Lippard, S. J. *J. Am. Chem. Soc.* **1984**, *106*, 5430–5439.

(14) Hollis, L. S.; Roberts, M. M.; Lippard, S. J. *Inorg. Chem.* **1983**, *22*, 3637–3644.

(15) Miskowski, V. M.; Schaefer, W. P.; Sadeghi, B.; Santarsiero, B. D.; Gray, H. B. *Inorg. Chem.* **1984**, *23*, 1154–1162.

Contribution No. 7489 from the Arthur Amos Noyes Laboratory, California Institute of Technology,
Pasadena, California 91125, and Mechanical and Chemical Systems Division, Jet Propulsion Laboratory,
California Institute of Technology, Pasadena, California 91109

Electronic Spectroscopy of d^8–d^8 Diplatinum Complexes. $^1A_{2u}(d\sigma^* \rightarrow p\sigma)$, $^3E_u(d_{xz},d_{yz} \rightarrow p\sigma)$, and $^{3,1}B_{2u}(d\sigma^* \rightarrow d_{x^2-y^2})$ Excited States of $Pt_2(P_2O_5H_2)_4^{4-}$

Albert E. Stiegman,[†] Steven F. Rice,[†] Harry B. Gray,*[†] and Vincent M. Miskowski*[‡]

Received September 24, 1986

Polarized electronic spectral measurements have been made on single crystals of $(n\text{-}Bu_4N)_4[Pt_2(P_2O_5H_2)_4]$, and the solution photophysical properties of the $^1A_{2u}(d\sigma^* \rightarrow p\sigma)$ excited state have been studied. The $^{1,3}A_{2u}(d\sigma^* \rightarrow p\sigma)$ excited states have closely comparable excited-state distortions (largely a metal–metal contraction). Absorptions near 35 000 cm^{-1} attributable to transitions to singlet and triplet $d\sigma^* \rightarrow d_{x^2-y^2}$ excited states have been identified by their polarizations and large half-widths. Bands assigned to triplet components of $d_{xz},d_{yz} \rightarrow p\sigma$ excitations are at slightly higher energy; the extreme narrowness (500 cm^{-1} for the transition to $E_u(^3E_u)$) of these absorption systems indicates that the excited states in question are not distorted.

Numerous spectroscopic and photophysical studies on $Pt_2(P_2O_5H_2)_4^{4-}$ (D_{4h} Pt_2P_8 coordination unit) have appeared recently.[1-3] Of primary interest has been the long-lived (9.8 μs for room-temperature aqueous solution[1b]) and highly emissive $^3A_{2u}(d\sigma^* \rightarrow p\sigma)$ excited state with some attention[1c,d] also given to the weakly luminescent $^1A_{2u}(d\sigma^* \rightarrow p\sigma)$ state. Remarkable photochemistry has been observed[3,4] for the $^3A_{2u}$ excited state of this d^8–d^8 Pt_2 species.

With the aim of elucidating the $^1A_{2u}$ and other upper excited states, we have prepared and characterized the $n\text{-}Bu_4N^+$ salt of $Pt_2(P_2O_5H_2)_4^{4-}$. Extremely thin crystals of this compound are readily obtained, and polarized electronic absorption measurements

---

[†] Arthur Amos Noyes Laboratory.
[‡] Jet Propulsion Laboratory.

(1) (a) Fordyce, W. A.; Brummer, J. G.; Crosby, G. A. *J. Am. Chem. Soc.* **1981**, *103*, 7061–7064. (b) Che, C.-M.; Butler, L. G.; Gray, H. B. *J. Am. Chem. Soc.* **1981**, *103*, 7796–7797. (c) Rice, S. F.; Gray, H. B. *J. Am. Chem. Soc.* **1983**, *105*, 4571–4575. (d) Bär, L.; Gliemann, G. *Chem. Phys. Lett.* **1984**, *108*, 14–17. (e) Isci, H.; Mason, W. R. *Inorg. Chem.* **1985**, *24*, 1761–1765.

(2) Shimizu, Y.; Tanaka, Y.; Azumi, T. *J. Phys. Chem.* **1984**, *88*, 2423–2425.

(3) (a) Heuer, W. B.; Totten, M. D.; Rodman, G. S.; Hebert, E. J.; Tracy, H. J.; Nagle, J. K. *J. Am. Chem. Soc.* **1984**, *106*, 1163–1164. (b) Bryan, S. A.; Dickson, M. K.; Roundhill, D. M. *J. Am. Chem. Soc.* **1984**, *106*, 1882–1883. (c) Peterson, J. R.; Kalyanasundaram, K. *J. Phys. Chem.* **1985**, *89*, 2486–2492.

0020-1669/87/1326-1112$01.50/0

Table I. Absorption Maxima of $Pt_2(P_2O_5H_2)_4^{4-}$

	soln of K^+ salt in H_2O (25 °C)		soln of n-Bu_4N^+ salt in CH_3CN (25 °C)		n-Bu_4N^+ salt, single cryst at 15 K	
$^1A_{1g} \rightarrow$	λ_{max}, nm	ϵ	λ_{max}, nm	ϵ	λ_{max}, nm	π/σ polarization ratio
$E_u(^3A_{2u})$, $d\sigma^* \rightarrow p\sigma$	452	110	453	155	456	0.6
$^1A_{2u}$, $d\sigma^* \rightarrow p\sigma$	367	34 500	372	33 400	370	>25
$E_u(^3B_{2u})$, $d\sigma^* \rightarrow d_{x^2-y^2}$	305	990	315	1640	313	~0.5[a]
$^1B_{2u}$, $d\sigma^* \rightarrow d_{x^2-y^2}$	266	1550	285	2550	286	~1.5[a]
$E_u(^3E_u)$, $d_{xz},d_{yz} \rightarrow p\sigma$	243	3350	246	3770	250	0.55
$A_{2u}(^3E_u)$, $d_{xz},d_{yz} \rightarrow p\sigma$	220	8700, sh	222	10 600, sh	222	>5
^1E_u, $d_{xz},d_{yz} \rightarrow p\sigma$	<200	>35 000	<200	>40 000	<215	<1

[a] After curve resolution from other overlapping absorptions.

in previously inaccessible spectral regions[1c] have been made. We also have investigated the photophysical properties of the $^1A_{2u}$ excited state.

Experimental Section

$K_4[Pt_2(P_2O_5H_2)_4]$ was prepared as described previously.[1c] The n-Bu_4N^+ salt was obtained by dissolving 0.25 g of $K_4[Pt_2(P_2O_5H_2)_4]$ in a minimum amount of water (~50 mL) and extracting with 50 mL CH_2Cl_2 containing an excess of (n-Bu_4N)Cl. (n-Bu_4N)$_4$[$Pt_2(P_2O_5H_2)_4$] was precipitated from the organic layer by addition of a minimum amount of anhydrous ether, filtered, and dried. The extraction was carried out under low light to prevent photodecomposition in the CH_2Cl_2 solvent. Anal. Calcd (found) for $C_{64}H_{152}N_4O_{20}P_8Pt_2$: C, 39.71 (38.57); H, 7.91 (7.61); N, 2.89 (2.84).

Acetonitrile obtained from Burdick and Jackson was degassed with multiple freeze–pump–thaw cycles, distilled, and stored over activated alumina. Dichloromethane (also from Burdick and Jackson) was used as received.

Instrumentation for emission lifetime measurements and low-temperature electronic spectroscopy has been described previously.[1c,5] Emission quantum yields were determined by using quinine sulfate (Aldrich) 1 M H_2SO_4(aq) as an emission standard. Picosecond emission lifetime data were obtained at the Center for Fast Kinetics, The University of Texas, Austin, TX. The fluorescence lifetime of $Pt_2(P_2O_5H_2)_4^{4-}$ in aqueous solution was close to the instrumental response function; however, comparison to standards with very short emission lifetimes indicated a real emission decay, and deconvolution gave an emission lifetime of 8 ps. Our experience with deconvolution procedures suggests that an uncertainty of ±5 ps should be attached to this value, even though the statistical uncertainty in the fit was only 0.5 ps.

(n-Bu_4N)$_4$[$Pt_2(P_2O_5H_2)_4$] proved to readily form thin crystals with face areas up to 1 cm^2 when solutions in CH_3CN were slowly evaporated onto quartz plates. Well-formed crystals were generally less than ~10 μm in thickness (thicker crystals were aggregates). Crystal thickness was controlled simply by adjusting concentration, as solubility is high and crystals form only upon evaporation of all solvent.

We were able to form extremely thin crystals (sufficient to keep absorption bands of isotropic extinction coefficient ~35 000 on scale) by this technique. For thicker crystals, the crystal face that developed (the only one observed) showed very sharp (wavelength-independent) extinctions; moreover, studies of the polarizer angle dependence of the electronic spectra of such crystals showed absorption maxima and minima identical with the extinctions, independent of wavelength. This crystal face thus presumably contains an optic axis in a monoclinic (or higher) symmetry lattice.

For thicker crystals, single-crystal regions were picked out by selecting regions of uniform extinctions and interference colors and were carefully masked off. The thinnest crystals of this study were so thin that rotation of polarized visible light was very small, and extinctions were therefore hard to detect under the polarizing microscope. However, when such samples were tilted and reflected light was observed, variations in reflectivity suggested that certain regions might be single crystals. Careful masking to isolate these regions yielded a few samples with high ultraviolet absorption polarizations.

Results and Discussion

The electronic spectra of $Pt_2(P_2O_5H_2)_4^{4-}$ in aqueous and acetonitrile solutions are very similar (Figure 1, Table I), and absorption and emission maxima in CH_2Cl_2 solution are identical with those in CH_3CN. Most aqueous solution absorption maxima are only slightly red-shifted in CH_3CN, except the weak, broad peak at 266 nm in H_2O, which strongly red-shifts to 285 nm (a 2500-cm^{-1} shift) in the less polar solvent. A weaker band at longer wavelength (305 nm in H_2O) also seems to red-shift, but the resolution of this feature from surrounding intense absorptions is poor. The small solvent shifts for the $^{1,3}A_{2u}$ absorption bands argue against axial coordination of solvent in the ground state, because the electronic transitions in question are purely axial. Similar independence of emission maxima[1,3c] also excludes axial coordination in the $^{1,3}A_{2u}$ excited states.

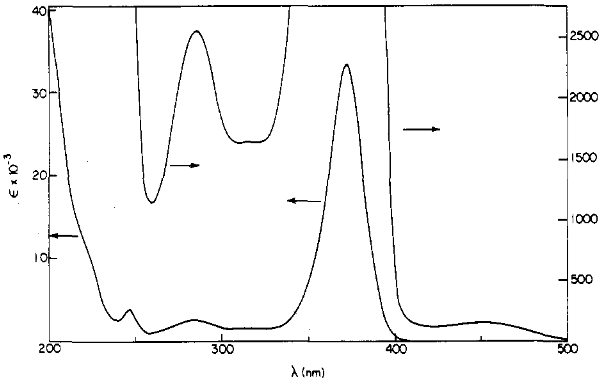

Figure 1. Electronic absorption spectrum of (n-Bu_4N)$_4$[$Pt_2(P_2O_5H_2)_4$] in CH_3CN solution at room temperature.

Table II. Photophysical Data for $Pt_2(P_2O_5H_2)_4^{4-}$

	phosphorescence			fluorescence		
solvent	τ_P, μs	ϕ_P	$10^{-4}(k_r)_P$, s^{-1}	τ_F, ps	$10^4\phi_F$	$10^{-7}(k_r)_F$, s^{-1}
H_2O	9.8	0.52	5.3	~8	1.6	2
CH_3CN	9.4	0.61	6.5	*a*	1.5	

[a] Not determined.

Photophysical Parameters. Table II summarizes photophysical data for $Pt_2(P_2O_5H_2)_4^{4-}$ in aqueous and CH_3CN solutions. We have experienced some of the reported[3c] difficulties with measurements in CH_3CN solution but find reproducible behavior in rigorously pure solvent. We are not aware of any previous photophysical data for the $^1A_{2u}$ fluorescence. The very low fluorescence yield relative to phosphorescence (~3 × 10^{-4}) is characteristic of well-degassed solutions in which $^3A_{2u}$ quenching by dioxygen is negligible. Enhanced spin–orbit coupling should promote $^1A_{2u}$/$^3A_{2u}$ intersystem crossing[6] in the Pt_2 system.

Radiative rate constants for the emissions are included in Table II. For comparison, we calculated k_r (Strickler-Berg[7]) on the basis of the absorption bands in H_2O solution, arriving at values of 4

---

(4) (a) Alexander, K. A.; Stein, P.; Hedden, D. B.; Roundhill, D. M. *Polyhedron* **1983**, *2*, 1389–1392. (b) Roundhill, D. M. *J. Am. Chem. Soc.* **1985**, *107*, 4354–4356. (c) Marshall, J. L.; Stiegman, A. E.; Gray, H. B. *ACS Symp. Ser.* **1986**, *No. 307*, 166–176.

(5) (a) Nocera, D. G.; Winkler, J. R.; Yocom, K. M.; Bordignon, E.; Gray, H. B. *J. Am. Chem. Soc.* **1984**, *106*, 5145–5150. (b) Hopkins, M. D.; Miskowski, V. M.; Gray, H. B. *J. Am. Chem. Soc.* **1986**, *108*, 959–963.

(6) (a) Winkler, J. R.; Marshall, J. L.; Netzel, T. L.; Gray, H. B. *J. Am. Chem. Soc.* **1986**, *108*, 2263–2266. (b) Miskowski, V. M.; Nobinger, G. L.; Kliger, D. S.; Hammond, G. S.; Lewis, N. S.; Mann, K. R.; Gray, H. B. *J. Am. Chem. Soc.* **1978**, *100*, 485–488.

(7) Porter, G. B. In *Concepts of Inorganic Photochemistry*; Adamson, A. W., Fleischauer, P. D., Eds.; Wiley-Interscience: New York, 1975; Chapter 2.

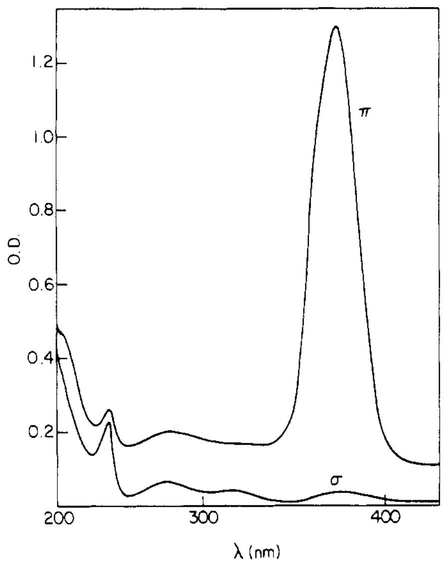

Figure 2. Polarized absorption spectra at room temperature of a very thin single crystal of $(n\text{-}Bu_4N)_4[Pt_2(P_2O_5H_2)_4]$. The π base line is vertically offset by 0.1 OD unit.

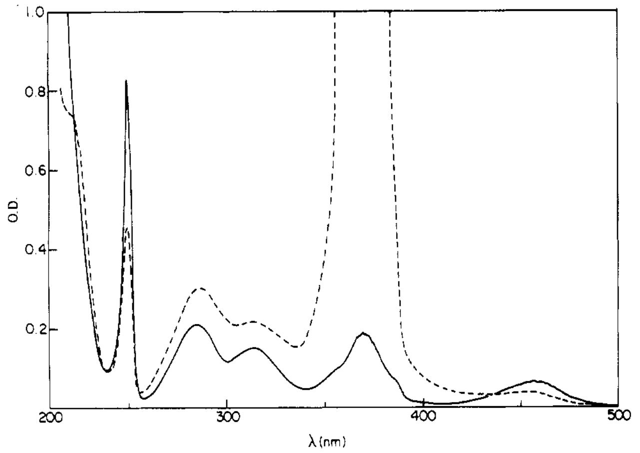

Figure 3. Polarized absorption spectra at 15 K of a thin single crystal of $(n\text{-}Bu_4N)_4[Pt_2(P_2O_5H_2)_4]$: (– –) π spectrum; (—) σ spectrum.

$\times 10^5$ s^{-1} (phosphorescence) and 1.5×10^8 s^{-1} (fluorescence). In both cases, these estimates are about 1 order of magnitude high and would therefore predict emission lifetimes (given the emission quantum yields) 10 times shorter than observed. Whatever the cause of the deviation,[8] the fact that it is similar for the $^{1,3}A_{2u}$ emissions supports the idea that the singlet and triplet excited states are electronically and geometrically similar.

Single-Crystal Spectroscopy. Representative single-crystal spectra for $(n\text{-}Bu_4N)_4[Pt_2(P_2O_5H_2)_4]$ are shown in Figures 2 and 3. All bands narrow sharply at low temperature. With the possible exception of the bands in the 250–350-nm region, which are not well resolved from stronger systems to shorter and longer wavelength at room temperature, integrated intensities are temperature independent.

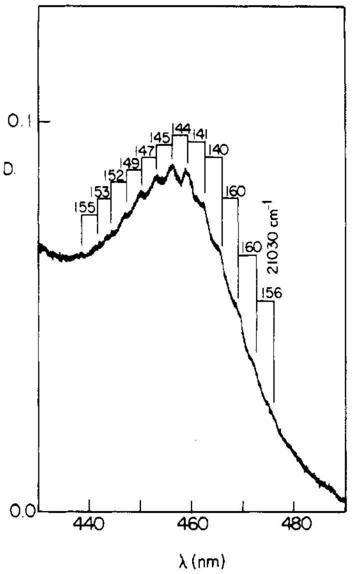

Figure 4. σ-Polarized absorption spectrum of a thick single crystal of $(n\text{-}Bu_4N)_4[Pt_2(P_2O_5H_2)_4]$. The average vibronic spacing is 150 cm^{-1}.

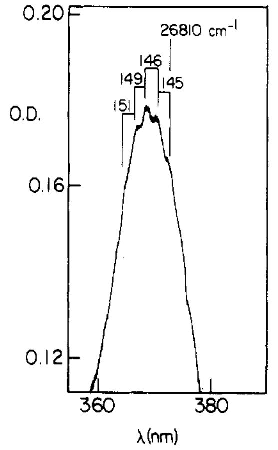

Figure 5. Expanded view of the vibronic structure near the $^1A_{1g} \rightarrow {}^1A_{2u}(d\sigma^* \rightarrow p\sigma)$ maximum in σ polarization for a thin crystal (Figure 3) at 15 K. The average vibronic spacing is 147 cm^{-1}.

The crystal structure of the $n\text{-}Bu_4N^+$ salt is not known. However, the crystal face studied is well-behaved optically, and the anion orientation can be inferred by comparison to published data[1c] on the crystallographically characterized potassium salt. It has been demonstrated[1c] that the ~370-nm band ($^1A_{1g} \rightarrow {}^1A_{2u}$, $d\sigma^* \rightarrow p\sigma$) is completely polarized parallel to the metal-metal axis. Our data (Figure 2) indicate that the intensity of this band is about a factor of 25 greater in one of the extinctions (hereafter designated π) than the other (designated σ). The projection of the metal–metal axis onto the crystal face therefore lies very near the π extinction.

The ~450-nm band ($^1A_{1g} \rightarrow E_u(^3A_{2u})$, $d\sigma^* \rightarrow p\sigma$) was found[1c] to be completely polarized perpendicular to the metal–metal axis. Our data (Figure 3, for example) indicate that this band has a σ/π polarization ratio of about 2. This suggests[1c] that the metal–metal axis is inclined at an angle of ~45° to the crystal face that was studied. This situation is very similar to that observed[1c] for the Ba^{2+} salt of $Pt_2(P_2O_5H_2)_4{}^{4-}$. Summarizing, we infer that the σ polarization is a nearly pure molecular x,y (perpendicular to metal–metal) spectrum, while π is a ~50/50 mixture of molecular x,y and z spectra. The isotropic spectrum should then be given by $\sim(2\pi + \sigma)/3$, and comparison of Figures 1 and 2 indicates this to be reasonable.

We first consider the distortions in the $^{1,3}A_{2u}(d\sigma^* \rightarrow p\sigma)$ excited states. Vibronic structure in these bands (Figures 4–6) is not nearly as well resolved as was previously reported[1c] for the $^3A_{2u}$ state of $Ba_2[Pt_2(P_2O_5H_2)_4]$. This is not unexpected for a $n\text{-}Bu_4N^+$

---

(8) In the case of the $^3A_{2u}$ emission, some deviation from the Strickler–Berg value is expected because the triplet state is a thermally equilibrated mixture of E_u and A_{1u} spin–orbit components (split by 41 cm^{-1}).[1] The electronic transition from the A_{1u} component is forbidden, so at high temperatures k_r(obsd) should be two-thirds of that for the allowed ($E_u \leftrightarrow A_{1g}$) transition. The phosphorescence lifetime is impressively temperature independent above liquid-nitrogen temperature, showing no deviation from the value of Table II in the temperature range 80–330 K. We additionally note that any contribution to the total fluorescence from delayed fluorescence (emission from singlets thermally back-populated from triplets) is not likely to be important, because of the large singlet–triplet splitting (5200 cm^{-1}) in both absorption and emission. With this value and the k_r value given in the text, we calculate ϕ(delayed fluorescence) = 1.6×10^{-9} compared with $\phi_f/\phi_p = 3 \times 10^{-4}$.

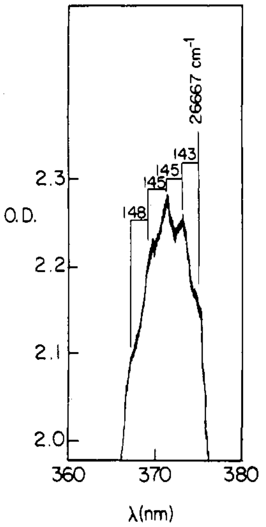

Figure 6. Vibronic structure near the $^1A_{1g} \rightarrow {}^1A_{2u}(d\sigma^* \rightarrow p\sigma)$ maximum in π polarization for a very thin crystal (Figure 2) at 15 K. The average vibronic spacing is 145 cm^{-1}.

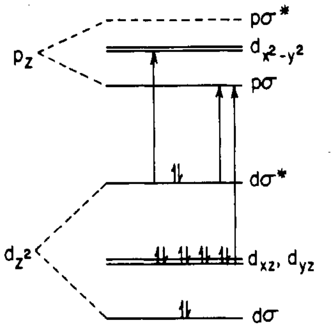

Figure 7. Molecular orbital diagram showing experimentally located electronic transitions for $Pt_2(P_2O_5H_2)_4^{4-}$. The d_{xz},d_{yz} orbitals should be split into $\pi(e_u)$ and $\pi^*(e_g)$ levels for a d^8–d^8 Pt_2 complex; however, no evidence for this splitting has been found.

salt, which has a pronounced proclivity toward crystallographic disorder; thus, some sort of multiple site or inhomogeneous broadening is likely operative.

Despite the low resolution, close similarity of the vibronic patterns of Figures 4–6 to that[1c] of $^3A_{2u}$ of the Ba^{2+} salt is apparent. The band half-widths are essentially identical (~1350 cm^{-1}), and progressions in ~150 cm^{-1} (155 cm^{-1} for $^3A_{2u}$ of the Ba^{2+} salt[1c]), which are attributable to the excited-state $\nu(Pt_2)$ mode, are evident.

Importantly, we conclude from the similiarity of bandwidths and excited-state vibrational frequencies that the singlet and triplet A_{2u} ($d\sigma^* \rightarrow p\sigma$) potential surfaces are virtually the same.[9] This is reasonable, because electron correlation effects are not expected to produce large electronic differences between the singlet and triplet states when the electronic transition is one such as $d\sigma^* \rightarrow p\sigma$. It may be noted that this result also excludes large spin–orbit mixing with higher energy states, since this would differ for $A_{2u}(^1A_{2u})$ and $E_u(^3A_{2u})$.

We now turn to the bands to higher energy of $^{1,3}A_{2u}$. The next intense band in the spectra of d^8–d^8 Rh_2 complexes has been assigned[10] to the molecular x,y-polarized $^1A_{1g} \rightarrow {}^1E_u(d_{xz},d_{yz} \rightarrow p\sigma)$ transition; this band is both very intense (ϵ 30 000–50 000) and narrow. The A_{2u} and E_u components of the transition to the ^3E_u state are observed[10b] as weaker lines to lower energy, with appropriate (z and x,y, respectively) polarizations.

We assign narrow z and x,y-polarized features in our spectra (Figure 3) at, respectively, 222 and 250 nm to the transitions to A_{2u} and $E_u(^3E_u)$. The data show that there must be a very intense x,y-polarized band to shorter wavelength of the experimental limit (which was ~200 nm (solution) or ~215 nm (crystal)) and we attribute this to the transition to $E_u(^1E_u)$. The extremely high energy inferred for this transition is consistent with the spectrum of a monomeric planar analogue, Pt(bis(diethylphosphino)-ethane)$_2^{2+}$, which shows[11] no intense bands below 210 nm. The observed ordering of the ^3E_u spin–orbit components ($A_{2u} > E_u$) is reasonable[2] from the viewpoint of spin–orbit coupling, since the intense singlet–singlet transitions to A_{2u} ($d\sigma^* \rightarrow p\sigma$) and $E_u(d_{xz},d_{yz} \rightarrow p\sigma)$ states fall below and above ^3E_u, respectively.

The extreme narrowness of the well-resolved $E_u(^3E_u)$ band (500 cm^{-1} at low temperature) is noteworthy. There obviously can be no large molecular distortions associated with this excitation. Analogous bands for d^8–d^8 Rh_2 complexes are similarly narrow.[10b] Why should the $d_{xz},d_{yz} \rightarrow p\sigma$ excitations be so vertical, and furthermore, why should they occur at nearly the same energies as the transitions of mononuclear analogues, as has been established for the Rh(I) complexes?[10]

It must be concluded that population of pσ does not change the metal–metal bond length, since progressions in $\nu(M_2)$(hence broader bands), analogous to the $d\sigma^* \rightarrow p\sigma$ excitations, would otherwise result. This may seem to be a surprising conclusion, since mixing of pσ (and pσ*) into the ground state has been invoked[10] to explain the weak ground-state metal–metal bonding. However, since pσ, which is formed from Pt 6p orbitals admixed with ligand π^* orbitals, is much more diffuse than dσ or dσ*, its optimal metal–metal bonding distance should be relatively large. We suggest that the ground-state metal–metal distance (2.925 Å)[12] may already be optimized for 6p interaction (as a result of the configuration interaction); in this case, the metal–metal distance would be insensitive to 6p population. An important consequence of this interpretation is that platinum–platinum bond lengths that result from oxidation (2.793 Å, $K_4[Pt_2(P_2O_5H_2)_4Br]\cdot 3H_2O$; 2.695 Å, $K_4[Pt_2(P_2O_5H_2)_4Cl_2]\cdot 2H_2O$)[13] or $d\sigma^* \rightarrow p\sigma$ excitation (2.71 Å)[1c] would reflect only the changes in dσ bonding.

We finally turn to the weak bands at 286 and 313 nm. The most striking observation is that they are very broad even at low temperature (half-widths ~3100 cm^{-1}). Because both bands are over twice as broad as $^{1,3}A_{2u}$ ($d\sigma^* \rightarrow p\sigma$), the most reasonable assignments are to transitions terminating in the empty Pt $d_{x^2-y^2}$ orbitals. Excited states of this type are strongly distorted along the metal–(equatorial ligand) stretching coordinate, and typically[14] show half-widths of 2000–4000 cm^{-1}.

The large solvent effect on λ_{max} of each of the broad bands can be rationalized in terms of the interaction of hydrogen-bonding solvents such as H_2O with the PO_2H groups, an interaction that would be expected to change the ligand-field strength of bridging pyrophosphite. As previously noted, there is no evidence for axial solvent interaction with the metal atoms, and the axial excitations such as $d\sigma^* \rightarrow p\sigma$ may therefore be less solvent sensitive.

The transitions in question evidently lie to higher energy of d → p excitations for monomeric Pt(II) complexes of strong-field ligands.[11,15] The logical candidates are those that originate in

---

(9) There appear to be shoulders on $^1A_{2u}$ in σ polarization at ~385 and ~355 nm (Figure 3). These are artifacts! This particular crystal showed a stray light (light leak) established maximum absorbance of 2.45 at low temperature for $^1A_{2u}$ in π polarization, and the edges of the "topped-off" band correspond to the shoulders in σ polarization. Such shoulders were not observed for crystals thin enough so that the $^1A_{2u}$ maximum in π polarization was not affected by stray light (e.g., Figure 2). The shoulders are therefore attributed to crystal misalignment, with the very intense topped-off π polarization leaking into σ polarization. It seems likely to us that weak x,y-polarized 350–400-nm bands previously reported[1c] for the K^+ and Ba^{2+} salts may similarly be artifacts. (It was noted[1c] that the intensities of these features were not reproducible.)

(10) (a) Mann, K. R.; Thich,J. A.; Bell, R. A.; Coyle, C. A.; Gray, H. B. *Inorg. Chem.* **1980**, *19*, 2462–2468. (b) Rice, S. F. Ph.D. Thesis, California Institute of Technology, 1982. (c) Mann, K. R.; Gray, H. B. *Adv. Chem. Ser.* **1979**, *No. 173*, 225–235.

(11) Kozelka, J.; Lüthi, H.-P.; Dubler, E.; Kunz, R. W. *Inorg. Chim. Acta* **1984**, *86*, 155–163.

(12) Marsh, R. E.; Herbstein, F. H. *Acta Crystallogr. Sect. B: Struct. Sci.* **1983**, *B39*, 280–287.

(13) Che, C.-M.; Herbstein, F. H.; Schaefer, W. P.; Marsh, R. E.; Gray, H. B. *J. Am. Chem. Soc.* **1983**, *105*, 4604–4607.

(14) Eyring, G.; Schmidtke, H. H. *Ber. Bunsenges. Phys. Chem.* **1981**, *85*, 597–603.

the dσ* orbital, because these should be red-shifted significantly in d^8–d^8 Pt_2 species. The d$\sigma^* \rightarrow d_{x^2-y^2}$ excitations, $^1A_{1g} \rightarrow {}^{1,3}B_{2u}$ and $^{1,3}B_{1g}$, include just one dipole-allowed transition, that to $E_u(^3B_{2u})$.

We suggest that the 313-nm band involves excitation to $E_u(^3B_{2u})$, as, taking account of the influence of absorption due to surrounding bands, it appears to be about twice as intense in σ as in π polarization, which is consistent with an x,y-dipole-allowed transition. Moreover, Isci and Mason's MCD data[1e] are consistent with a negative A term for this band in aqueous solution. (The interpretation of the data by Isci and Mason was different, but needs to be modified because of our other results.)

The 286-nm band appears to be just slightly more intense in π polarization than in σ. This is not consistent with either molecular z or x,y polarization. The MCD data show only a B term[1e] coincident with the absorption maximum. The mixed polarization behavior suggests that the intensity may be vibronically induced and that the band may represent an orbitally forbidden transition to one or more of the singlet d–d states. In Table I we assign the band to $^1A_{1g} \rightarrow {}^1B_{2u}$, as the inferred $^{1,3}B_{2u}$ splitting is reasonable for a d–d transition.[16]

Comparison to Other Work. Isci and Mason have presented MCD data for $Pt_2(P_2O_5H_2)_4{}^{4-}$ in aqueous solution.[1e] Our results are generally compatible with theirs; in particular, they found a distinct A term for the ~250-nm band, consistent with our assignment to $^1A_{1g} \rightarrow E_u(^3E_u)$. Comparison to the spectra of d^8–d^8 Rh_2 compounds indicates[10] that the ~250-nm band is far weaker than expected for the singlet–singlet transition. With this change, all of Isci and Mason's assignments other than those for the $^{1,3}A_{2u}$(d$\sigma^* \rightarrow$ pσ) states need to be modified.

Our assignments (Figure 7 and Table I) also differ in detail from those proposed by Shimizu et al.,[2] which were based on fits to spin–orbit calculations. However, the energies of the $^{1,3}E_u(d_{xz},d_{yz} \rightarrow p\sigma)$ states are close to their predictions; as these states are the ones that determine the $A_{1u},E_u(^3A_{2u})$(d$\sigma^* \rightarrow$ pσ) spin–orbit splitting, the calculation of this splitting is reasonable.[2]

An interesting point is that we have been able to locate d–d excited states for $Pt_2(P_2O_5H_2)_4{}^{4-}$: states of this type have been postulated[17] to be important in thermally activated nonradiative decay of Rh(I) binuclear compounds. Our results provide a benchmark example that will aid in the estimation of the energies of d–d states in other d^8–d^8 species. For $Pt_2(P_2O_5H_2)_4{}^{4-}$ itself, the d–d states are clearly much too energetic to be accessible thermally from the emissive $^{1,3}A_{2u}$ states.

Acknowledgment. Assistance from the staff of the Center for Fast Kinetics Research (supported jointly by the Biotechnology Branch of the Division of Research Resources of NIH (Grant RR00886) and The University of Texas at Austin) is gratefully acknowledged. This research was supported by National Science Foundation Grant CHE84-19828 and the Caltech President's Fund.

Registry No. $(n\text{-}Bu_4N)_4[Pt_2(P_2O_5H_2)_4]$, 89462-52-2.

---

(15) Cowman, C. D.; Gray, H. B. *Inorg. Chem.* **1976**, *15*, 2823–2824.

(16) Tuszynski, W.; Gliemann, G. *Z. Naturforsch., A: Phys., Phys. Chem., Kosmophys.* **1979**, *34A*, 211–219.

(17) Rice, S. F.; Milder, S. J.; Gray, H. B.; Goldbeck, R. A.; Kliger, D. S. *Coord. Chem. Rev.* **1982**, *43*, 349–354.

Contribution from the Department of Chemistry, The University of North Carolina, Chapel Hill, North Carolina 27514,
and Laboratory of Chemical Biodynamics, Lawrence Berkeley Laboratory, University of California, Berkeley, California 94720

Intramolecular Electron Transfer in the Reductive Chromophore–Quencher Complex $[(bpy)Re(CO)_3(py\text{-}PTZ)]^+$

Pingyun Chen,[†] T. David Westmoreland,[†] Earl Danielson,[†] Kirk S. Schanze,[‡] Doug Anthon,[‡]
Paul E. Neveux, Jr.,[†] and Thomas J. Meyer*[†]

Received June 16, 1986

Three metal complexes containing the reductive quencher ligand py-PTZ, $[(bpy)Re(CO)_3(py\text{-}PTZ)]^+$ and $[(bpy)_2Ru^{II}L(py\text{-}PTZ)]^{n+}$ (where L = Cl^- (n = 1) and acetonitrile (n = 2)), were prepared and their redox and spectral properties investigated. The chromophore–quencher complexes have essentially the same photophysical properties as their corresponding pyridine analogues at 77 K in a 4:1 (v/v) ethanol/methanol glass, but their properties are profoundly different in fluid solution. For the Re complex in fluid solution excitation of the Re → π^*(bpy) metal to ligand charge-transfer (MLCT) chromophore at 355 nm is followed by rapid (<10 ns) appearance of transient absorption (TA) features at 350 and 500 nm consistent with formation of the charge-separated state $[(bpy^{\bullet-})Re(CO)_3(py\text{-}PTZ^{\bullet+})]^{+*}$. Picosecond TA experiments monitored at 500 nm show that the $PTZ^{\bullet+}$ site grows in within ~200 ps in polar organic solvents following laser excitation at 355 nm. The transient behavior observed leads to the conclusion that initial excitation of the MLCT chromophore is followed by rapid intramolecular electron-transfer quenching with $k_q(RT) = 4.8 \times 10^9\ s^{-1}$ in acetonitrile to give the charge-separated excited state $[(bpy^{\bullet-})Re(CO)_3(py\text{-}PTZ^{\bullet+})]^+$, which, in turn, decays to the ground state with $k_2 = 4.0 \times 10^7\ s^{-1}$.

Introduction

Oxidative- and reductive-electron-transfer quenching of the metal to ligand charge-transfer (MLCT) excited states of $Ru(bpy)_3{}^{2+}$ (bpy is 2,2′-bipyridine) and related complexes are well-defined processes, e.g., eq 1[1] (PQ^{2+} is N,N'-dimethyl-4,4′-bipyridinium ion; PTZ is phenothiazine).

$$
\begin{aligned}
&Ru(bpy)_3{}^{2+} + h\nu \rightarrow Ru(bpy)_3{}^{2+*} \\
&Ru(bpy)_3{}^{2+*} + PQ^{2+} \rightarrow Ru(bpy)_3{}^{3+} + PQ^{\bullet+} \qquad (1) \\
&Ru(bpy)_3{}^{2+*} + PTZ \rightarrow Ru(bpy)_3{}^{+} + PTZ^{\bullet+}
\end{aligned}
$$

A detailed understanding of the electron-transfer events that occur during and after the quenching step is restricted by the absence of structural information, which is an inherent limitation given the outer-sphere nature of the electron-transfer reactions involved.[1e,2] In part to

---

[†] The University of North Carolina.

[‡] University of California.

(1) (a) Meyer, T. J. *Acc. Chem. Res.* **1978**, *11*, 94. (b) Kalyanasundaran, K. *Coord. Chem. Rev.* **1982**, *46*, 159. (c) Al-Saigh, H. Y.; Kemp, T. J. *J. Chem. Res., Miniprint* **1984**, 2001. (d) Whitten, D. G. *Acc. Chem. Res.* **1980**, *13*, 83. (e) Sutin, N.; Creutz, C. *Pure Appl. Chem.* **1980**, *52*, 2717. (f) Balzani, V.; Bolletta, F.; Gandolfi, M. T.; Maestri, M. *Top. Curr. Chem.* **1978**, *75*, 1.

(2) (a) Meyer, T. J. *Prog. Inorg. Chem.* **1983**, *30*, 389. (b) Newton, M. D.; Sutin, N. *Annu. Rev. Phys. Chem.* **1984**, *35*, 437. (c) Isied, S. S. *Prog. Inorg. Chem.* **1984**, *32*, 443. (d) Haim, A. *Prog. Inorg. Chem.* **1983**, *30*, 273. (e) Balzani, V.; Scandola, F. In *Energy Resources Through Photochemistry and Catalysis*; Grätzel, M., Ed.; Academic: New York, 1983; Chapter 1.

0020-1669/87/1326-1116$01.50/0